On-Chip 4×10 GBaud/s Mode-Division Multiplexed PAM-4 Signal Transmission

Weifeng Zhang, *Member, IEEE*, Houman Ghorbani, Tong Shao, *Member, IEEE*, and Jianping Yao, *Fellow, IEEE*

***Abstract*—Emerging 5G mobile networks and cloud computing applications are driving the demand for an ever-increasing capacity of short-reach optical communications. To meet this demand, mode-division multiplexing (MDM) has been proposed to scale up the bandwidth density by leveraging the spatial modes of an optical waveguide for transmitting multiple optical signals. On the other hand, the use of multi-level pulse amplitude modulation (PAM) can also increase the transmission bandwidth. Therefore, on-chip MDM in conjunction with PAM is an approach to enhance the transmission capacity in a photonic integrated circuit. In this paper, we report a silicon photonic integrated four-channel MDM circuit for high data rate on-chip communications with a low channel crosstalk and small insertion loss. To make the circuit have a small size that supports broadband operation, a mode multiplexer and demultiplexer are realized with the use of cascaded asymmetrical directional couplers on rib waveguides. By incorporating the MDM circuit in an optical communications system, the transmission of a 4 x 10 GBaud/s OOK and PAM-4 signal is experimentally demonstrated. The performance in terms of eye diagrams and power penalties is evaluated. The power penalties for the four-channel OOK transmission are 4.31, 2.38, 1.44 and 3.5 dB at a BER of 10^{-9}. For the four-channel PAM-4 transmission, the power penalties are 7.98, 1.10, 0.66 and 5.14 dB. The required received optical power at a BER ($<3.8 \times 10^{-3}$) of the 7% overhead-hard decision FEC is −2.6 dBm. The key advantage of the approach is that high-capacity on-chip communications is enabled by the photonic integrated MDM circuit with a small footprint. Since the MDM circuit is implemented on a silicon photonic platform, the system holds high potential for full integration on a single chip.**

***Index Terms*—Mode-division multiplexing, pulse amplitude modulation, directional coupler, silicon photonics.**

I. Introduction

The amount of data generated in our daily life has grown exponentially in the past few years, which drives the need for an ever-increasing transmission capacity of communications systems. To meet the needs for higher data rate communications, novel transmission techniques including wavelength-division multiplexing (WDM), polarization-division multiplexing (PDM), higher-order modulation formats, and advanced digital signal processing techniques have been proposed and employed [1]–[5].

More recently, mode-division multiplexing (MDM) technique has been proposed and extensively studied since it offers an additional dimension of freedom for multiplexing to increase the bandwidth by leveraging the spatial modes of a waveguide to carry multiple optical signals [6]–[18]. Thanks to its favorable compatibility with WDM and PDM systems, the MDM technique provides an effective solution to scale up the bandwidth density of an existing network [19]–[21]. To realize MDM, a mode multiplexer and demultiplexer are required to multiplex and demultiplex effectively multiple signals with different modes. A few techniques have been reported, including the use of Y-branches [22], [23], asymmetrical directional couplers [24], [25], multimode interference couplers [26], [27], Mach–Zehnder interferometers [28], [29], and micro-ring resonators (MRRs) [30], [31]. In particular, an on-chip MDM-WDM optical communications system based on MRRs was experimentally demonstrated [31], in which an aggregate data rate up to 4.35 Tbit/s with 5 spatial modes and 87 WDM channels were supported. Due to the frequency selectivity nature of an MRR, the bandwidth is inherently limited, restricting the capability in further increasing the data rate of an MRR channel. On the contrary, mode multiplexers and demultiplexers implemented based on asymmetrical directional couplers do not have such a limit. Its operation bandwidth is much wider due to the nature of evanescent coupling between waveguides. In addition, the fabrication tolerance is much higher. Therefore, mode multiplexers and demultiplexers based on asymmetrical directional couplers are highly preferred. In the mode multiplexers and demultiplexers, mode converters are key components, which realize mode conversion based on three main physical mechanisms, including evanescent coupling, mode evolution, and multimode interferometry. Mostly, evanescent coupling is implemented by means of directional couplers [24] and ring resonators [31], mode evolution employs Y-junctions [32], and multimode interferometry is realized with the use of multimode interference (MMI) couplers [33].

On the other hand, the data capacity can also be increased by using higher-order modulation formats. For example, 4-level pulse amplitude modulation (PAM-4) offers four amplitude levels in one symbol and thus its bit rate is twice as high as on-off keying (OOK) at a same baud rate. Recently, a transmission system with an aggregate data rate of 192 Gbit/s based on on-chip three-mode multiplexing in conjunction with PAM-4

Manuscript received June 5, 2019; revised November 21, 2019 and December 29, 2019; accepted December 30, 2019. Date of publication January 6, 2020; date of current version February 6, 2020. This work was supported in part by the Natural Science and Engineering Research Council of Canada (NSERC) through the CREATE program and the CMC Microsystems, and in part by the NSERC under the Silicon Electronic-Photonic Integrated Circuits CREATE Program. *(Corresponding author: Jianping Yao.)*

The authors are with the Microwave Photonics Research Laboratory, School of Electrical Engineering and Computer Science, University of Ottawa, Ottawa, ON K1N 6N5, Canada (e-mail: wzhan088@uottawa.ca; hghor044@uottawa.ca; tong.shao03@gmail.com; jpyao@eecs.uottawa.ca).

Color versions of one or more of the figures in this article are available online at http://ieeexplore.ieee.org.

Digital Object Identifier 10.1109/JSTQE.2020.2964388

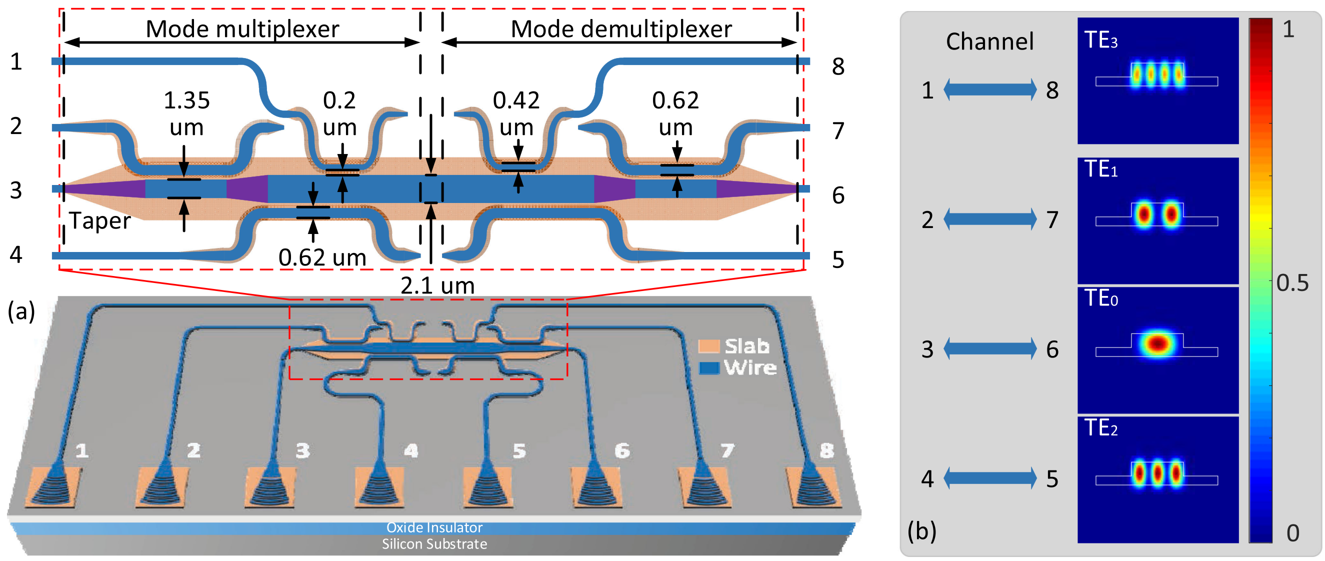

Fig. 1. (a) Schematic layout of the proposed silicon-based on-chip four-channel MDM circuit (Inset: zoom-in view of the waveguide configuration of the mode multiplexer and demultiplexer); and (b) simulated mode field profiles at the cross-section of a multi-mode bus waveguide.

has been reported [34]. The main problem with the on-chip mode multiplexer reported in [34] is the large footprint due to the use of wire waveguides. Compared with a wire waveguide, a rib waveguide has a much smaller propagation loss and stronger coupling coefficient, which is of great benefit to making a mode multiplexer and demultiplexer with a small footprint and low insertion loss.

In this paper, we report the design, fabrication and evaluation of a silicon photonic integrated four-channel MDM circuit and its use to achieve mode-division multiplexing for on-chip data transmission. The MDM circuit consists of a mode multiplexer and demultiplexer connected by a bus waveguide. To make the MDM circuit have a small size and support broadband operation, the mode multiplexer and demultiplexer are realized with the use of cascaded asymmetrical directional couplers on rib waveguides. By incorporating the fabricated MDM circuit in an optical communications system, high data rate on-chip data transmission is demonstrated. In the experiment, the transmission of 4×10 GBaud/s on-chip MDM OOK and PAM-4 signals is implemented. The performance of the system is evaluated by measuring the eye diagrams and the power penalties. For OOK transmission, the power penalties for the 4 channels are 4.31, 2.38, 1.44 and 3.5 dB at a BER of 10^{-9}. For PAM-4 transmission, the power penalties are 7.98, 1.10, 0.66 and 5.14 dB, and the required received optical power at a bit error rate (BER$<$ 3.8E-3) of the 7% overhead-hard decision forward error correction (FEC) is -2.6 dBm.

Note that a MDM was reported in 2018 by Dai *et al.* in [35]. Compared with the MDM in [35], the device reported in this paper is fabricated based on rib waveguides, which holds key advantages including smaller size and lower loss since a rib waveguide has a larger coupling coefficient and a smaller propagation loss than a wire waveguide.

The key advantage of the proposed technique is that high data capacity on-chip communications is enabled by the photonic integrated MDM circuit which has a small footprint and low insertion loss. Since the MDM circuit is implemented on a silicon photonic platform, the demonstrated short-reach communications system can be potentially integrated on a single chip.

II. On-Chip MDM Circuit

Fig. 1(a) shows the schematic of the proposed silicon-based on-chip MDM circuit to support four TE-polarization-mode multiplexed operation. In the chip, four input optical signals are coupled into the chip via four input grating couplers (1$\sim$4) which are mode-multiplexed at a multiplexer consisting of three cascaded asymmetrical directional couplers on rib waveguides. After transmission over a bus waveguide, the four signals are demultiplexed to four single-mode signals and obtained at four output ports (5$\sim$8). To minimize the chip footprint and reduce the bending loss, a wire waveguide is mostly used to route an input optical signal, while to enable a stronger optical coupling and lower propagation loss in the cascaded directional couplers, rib waveguides are mostly employed with a slab waveguide height of 90 nm.

The inset in Fig. 1(a) gives a zoom-in view of the waveguide configuration of a mode multiplexer and demultiplexer, in which the multiplexer and demultiplexer have an identical design, but are placed in a reverse geometry. Between the multiplexer and demultiplexer, a four-mode bus waveguide with a length of 20 μm is used for data transmission. With a 3D finite-difference time-domain simulation, in the mode multiplexer, a bus waveguide with a width of 1.35 μm and a length of 40 μm supporting two modes and another bus waveguide with a width of 2.1 μm and a length of 60 μm supporting four modes are connected with an adiabatic taper for mode transition [36]. To couple an input fundamental mode into a higher-order mode in a bus waveguide, a narrow access waveguide is located close to the bus waveguide.

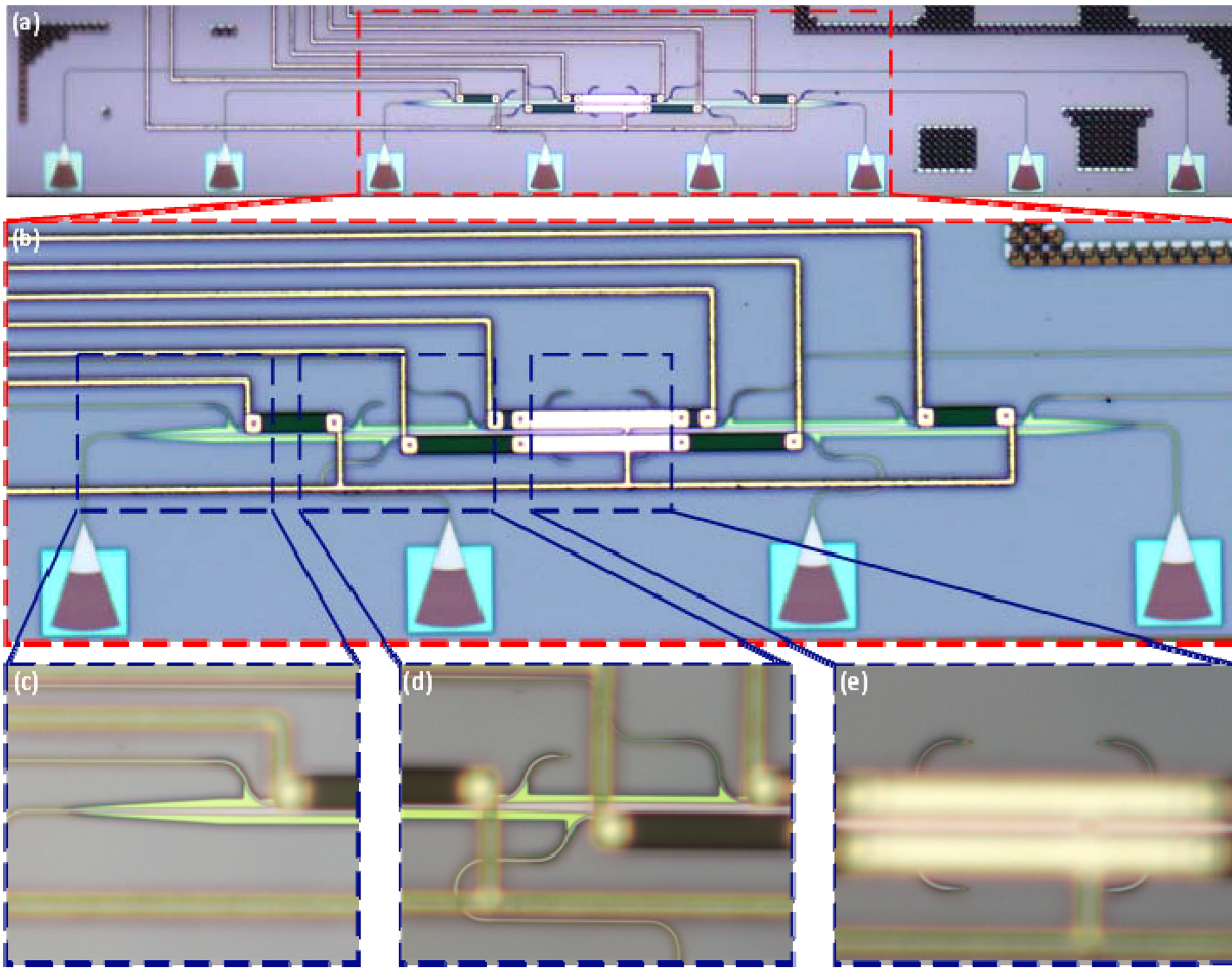

Fig. 2. (a) Prototyepe of the silicon-based on-chip four-channel MDM circuit; (b) zoom-in view of the waveguide structure for the mode multiplexer and demultiplexer; and (c)–(e) zoom-in views of the cascaded rib directional couplers.

To satisfy the phase-matching condition of evanescent coupling, the widths of three access waveguides are chosen to be 0.62, 0.62, and 0.42 μm, and to achieve a high coupling strength, the optimal coupling lengths for each mode are designed to be 34, 45, and 15 μm, with the identical coupling gap of 0.2 μm. In addition, at the end of the access waveguide, a waveguide terminator is used to radiate out the residual optical power. Fig. 1(b) shows the mode profiles at the cross-section of a four-mode bus waveguide in each mode channel. As can be seen, for the channel from port 1 to port 8, TE3 mode is supported, for the channel from port 2 to port 7, TE1 mode is supported, for the channel from port 3 to port 6, TE0 mode is supported, and for the channel from port 4 to port 5, TE2 mode is supported.

The device is fabricated using a CMOS-compatible technology with 193-nm deep ultraviolet lithography at IME, Singapore. The fabricated device has a size of 794 μm in length and 96 μm in width, giving a small footprint of 0.76 mm^2. The core area of the mode multiplexer and demultiplexer has a size of 340 μm in length and 37 μm in width, giving a small footprint of 0.13 mm^2. Fig. 2(a) is an image of the fabricated circuit captured by a microscope camera, and Fig. 2(b) gives a zoom-in view of the waveguide structure for the mode multiplexer and demultiplexer. On top of each directional coupler, an independent metallic micro-heater is placed for thermal tuning. Fig. 2(c)–(e) are zoom-in views of the three cascaded directional couplers on the rib waveguides in the mode multiplexer.

Then, the optical performance of the fabricated circuit is evaluated. Fig. 3(a)–(d) shows the transmission spectra at the four output ports (5∼8) when an input optical signal is launched to the circuit via the four input ports (1∼4) one at a time. The spectra are measured by an optical vector analyzer (LUNA OVA CTe). The transmitted optical power shown in Fig. 3 is normalized to the transmitted power at the wavelength of 1545 nm for the channel from port 1 to port 8. From the spectral measurement, the channel crosstalks resulted from the spatial mode multiplexing and demultiplexing are quantified. Table I presents the insertion loss and crosstalk in the different channels in Fig. 3 when an optical signal is launched into the chip

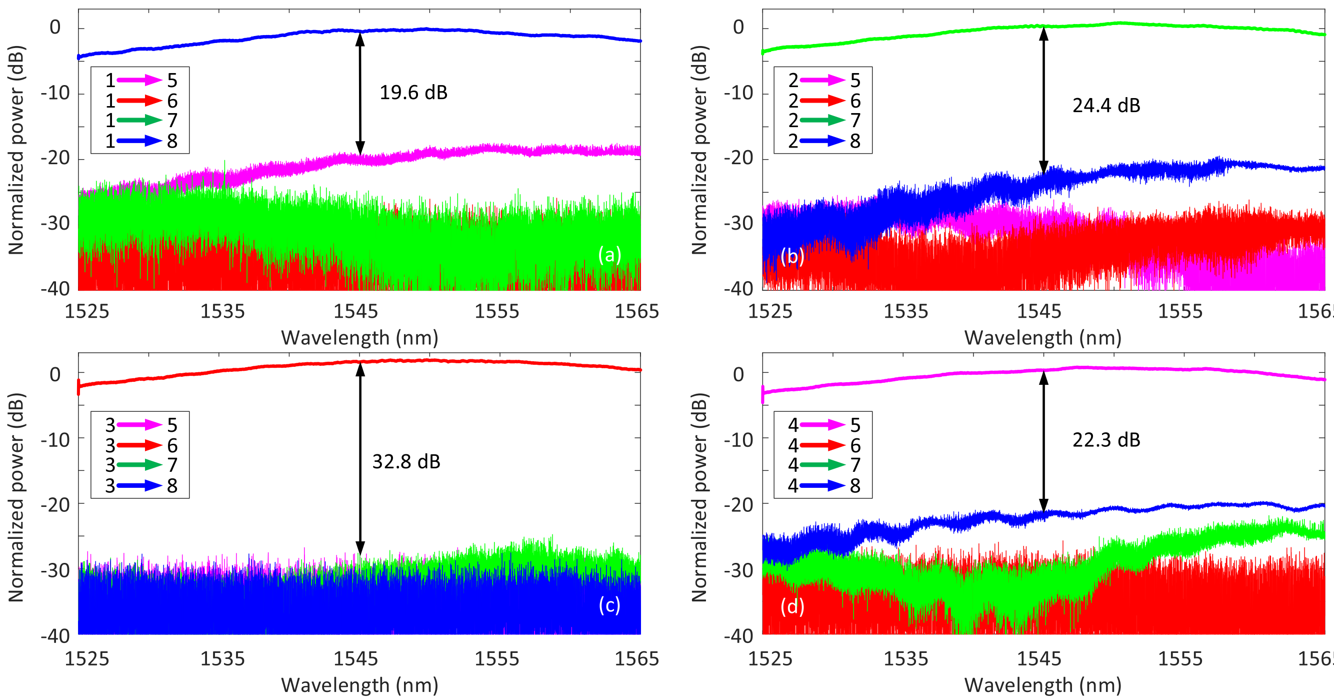

Fig. 3. Measured transmission spectra at the four output ports (5∼8) when the input optical signal is launched at the input port (a) 1, (b) 2, (c) 3, and (d) 4.

TABLE I
PROPERTIES OF THE MODE CHANNEL

Fig. 3	Input Port	Insertion loss* (dB) @ Output port	Crosstalk (dB)
(a)	PORT 1	12.6 @ PORT 8	19.6
(b)	PORT 2	10.2 @ PORT 7	24.4
(c)	PORT 3	9.4 @ PORT 6	32.8
(d)	PORT 4	10.3 @ PORT 5	22.3

*The insertion loss is measured at the incident wavelength of 1545 nm.

via different input port. The insertion losses for the different channels are slightly different due to the different coupling losses and mode propagation losses caused by the directional couplers in the channels. Based on the channel crosstalk measurements, the crosstalk for all channels are smaller than 19 dB, which confirms the effectiveness of the device to support four-mode-division multiplexing and demultiplexing operations. Note that the channel from port 3 to port 6 has the smallest crosstalk. This is because this channel guides the fundamental mode (TE0) without a directional coupler. The channels from port 1 to port 8 and from port 4 to port 5 have relatively higher crosstalk, which are caused due to the overlap of the coupling sections in the two directional couplers. By optimizing the coupler position design, the crosstalk between the two channels can be reduced.

III. ON-CHIP SIGNAL TRANSMISSION

An experiment to demonstrate the use of the fabricated circuit for MDM signal transmission is performed. Fig. 4 shows the experimental setup. An optical carrier from a tunable laser source (TLS, Anritsu MG9638A) is sent to an intensity modulator (IM, Lucent 2623CSA), where a PRBS 2^{13} signal with a data rate of 10-GBaud/s from an arbitrary waveform generator (AWG, Keysight M8195A) is applied to the IM to modulate the optical carrier. After amplification by an erbium-doped fiber amplifier (EDFA), the modulated optical signal is equally split into four channels. In each channel, a single mode fiber with a different fiber transmission length is used to ensure that the data are decorrelated between the channels. Then, the optical signal in each channel is launched via the corresponding input port to the chip. Note that a polarization controller (PC) is used to adjust the state of polarization of the input signal to minimize the polarization dependent loss. At the outputs of the chip, the demultiplexed signals are recovered one at a time with the use of a photodetector (PD, LR-12-A-M) and monitored by a sampling oscilloscope (Agilent 86116A) where the transmission performance is evaluated.

A. *OOK Signal Transmission*

First, the transmission of a 10-GBaud/s OOK signal is performed. The 10-GBaud/s OOK signal is generated by the AWG. Fig. 5(a) shows the measured bit error rates (BERs) of the OOK signal for back-to-back operation (B2B, without launching into the fabricated MDM circuit chip), single channel operation and four-mode MDM operation. For B2B, an optical power of −9 dBm is needed to ensure a BER of 10^{-9}. Compared with B2B, to maintain an identical BER of 10^{-9}, the optical powers needed are −8.69 dBm, −8.87 dBm, −8.93 dBm, and −8.77 dBm for single channel transmission from port 1 to port 8, port 2 to port

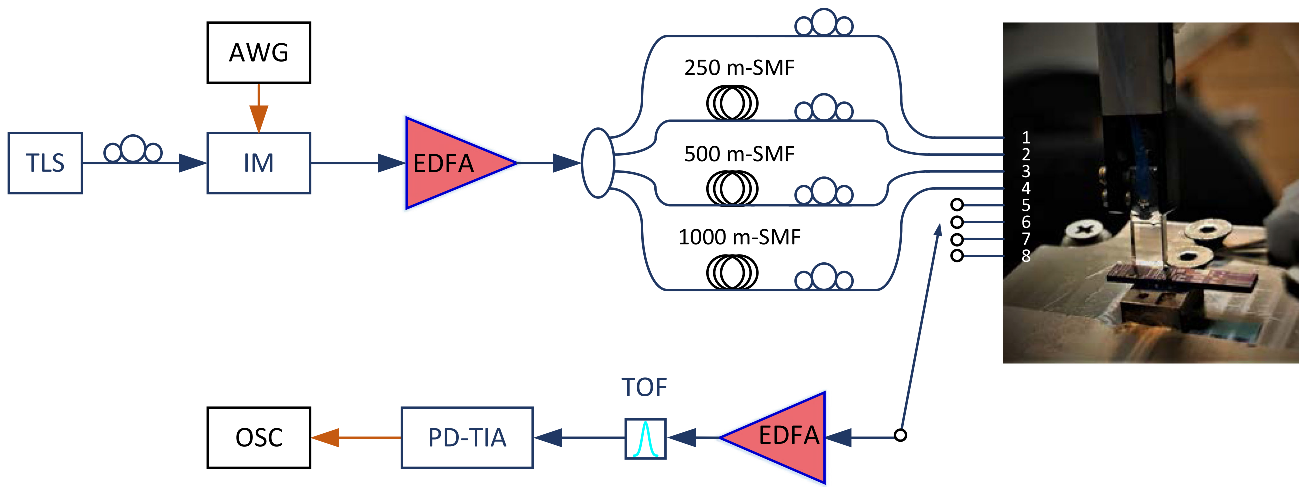

Fig. 4. Experimental setup for performance evaluation including a laser source, Arbitrary Waveform Generation (AWG), Intensity Modulator (IM), Erbium-Doped Fiber Amplifier (EDFA), Single-Mode Fiber (SMF), Tunable Optical Filter (TOF), Photodiode (PD-TIA), and Sampling oscilloscope (OSC).

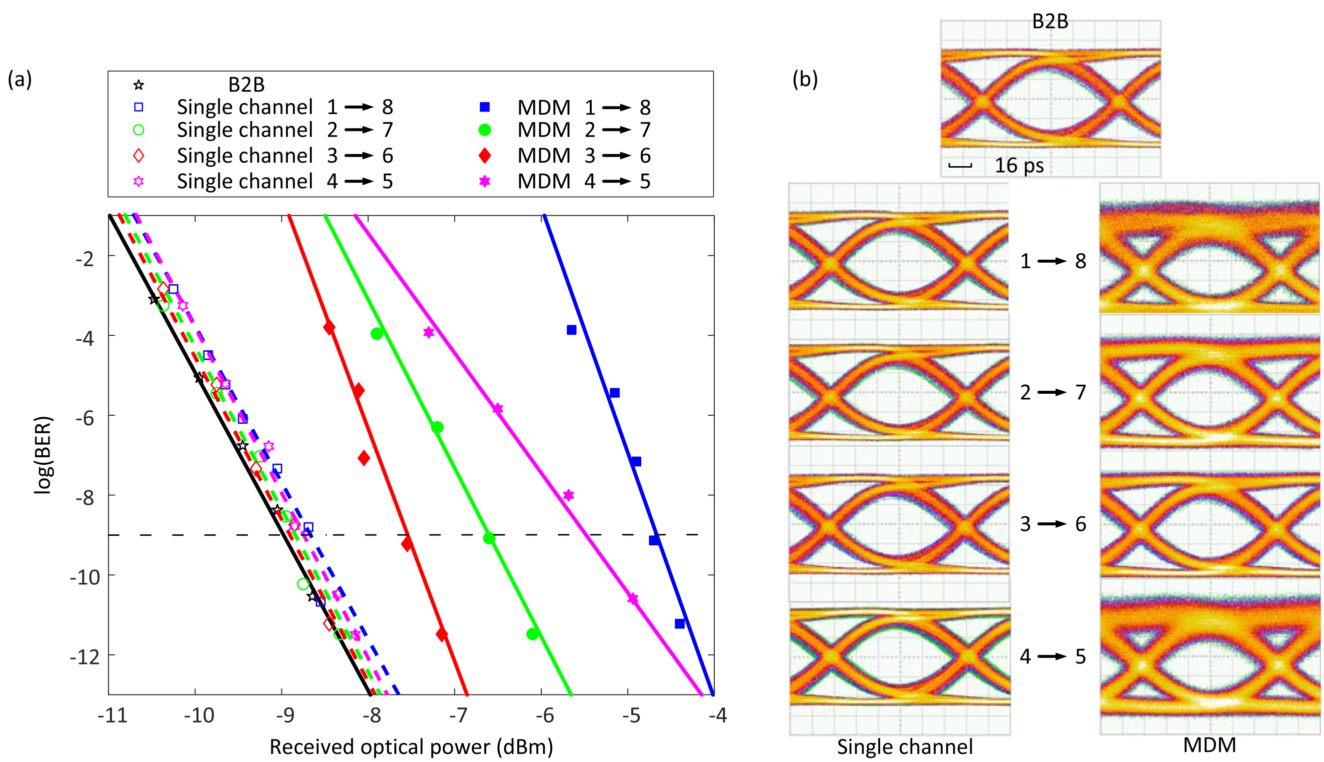

Fig. 5. (a) BER measurements for the transmission of an OOK signal for B2B, single port and MDM transmission for all the four channels; and (b) the eye diagrams for the four channels.

7, port 3 to port 6, and port 4 to port 5, with the corresponding power penalties of 0.31 dB on port 1, 0.13 dB on port 2, 0.07 dB on port 3 and 0.23 dB on port 4, respectively. For four-mode MDM operation, the power penalties are 4.31 dB from port 1 to port 8, 2.38 dB from port 2 to port 7, 1.44 dB from port 3 to port 6, and 3.5 dB from port 4 to port 5. Note that the B2B measurement is done by replacing the chip with a tunable attenuator to have an optical loss of 9.4 dB, which is identical to the insertion loss of the channel from port 3 to port 6. The higher power penalties from port 1 to port 8, and port 4 to port 5 are due to the stronger crosstalk, which leads to signal degradation in the channels. Fig. 5(b) shows the eye diagrams for B2B, single channel and four-mode MDM operation. Clear eye diagrams can be observed for B2B, single channel and MDM transmission,

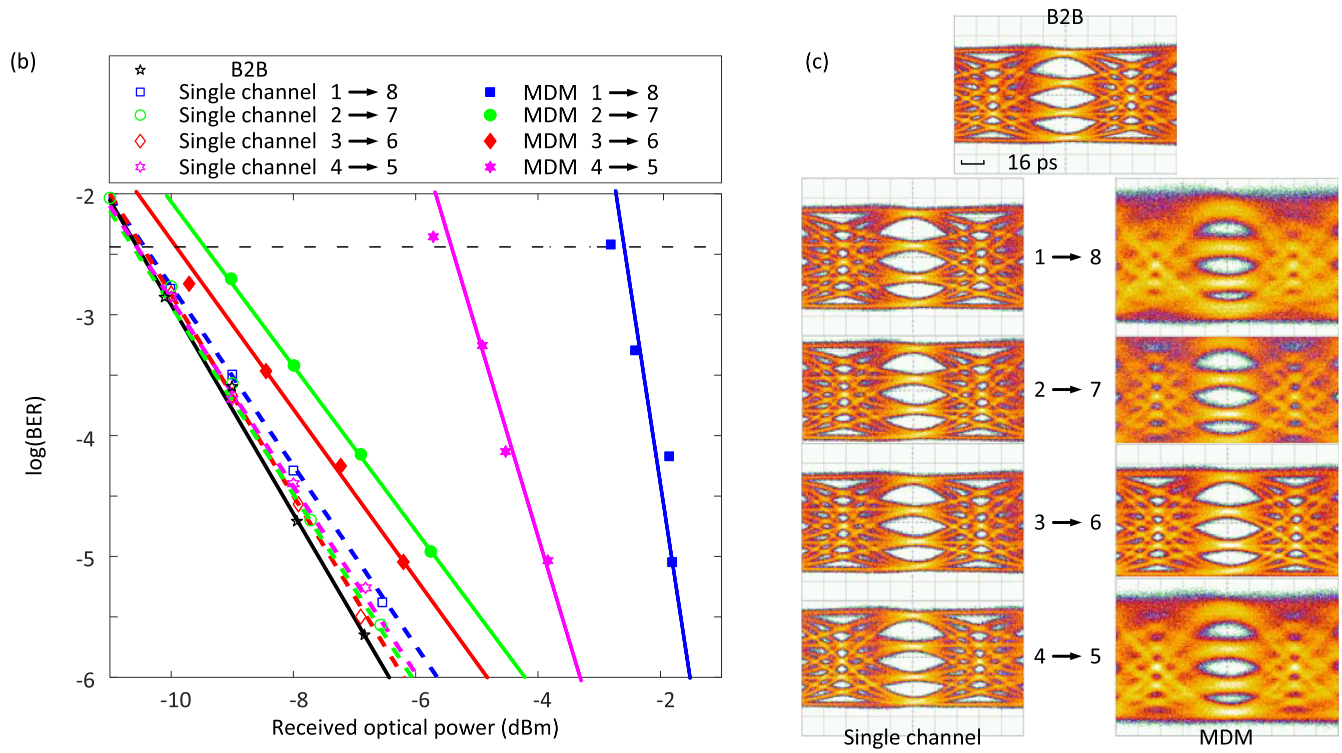

Fig. 6. (a) BER measurements for the transmission of a PAM-4 signal for B2B, single port and MDM transmission for all the four channels; and (b) the eye diagrams for the four channels.

which verifies the effectiveness of the system for MDM OOK signal transmission using the fabricated MDM circuit. The eyes for the channels from port 1 to port 8 and from port 4 to port 5 are relatively less opened, which are caused due to higher channel crosstalks.

B. PAM-4 Signal Transmission

Then, the transmission of a 10-GBaud/s PAM-4 signal is performed. Fig. 6(a) shows the measured BERs for B2B, single channel and the four-mode MDM operation. As can be seen, the 7% FEC threshold can be achieved when the received optical power is −2.2 dBm for the four-mode MDM operation. As can be seen, at a BER of 3.8×10^{-3}, the power penalties are 7.98 dB from port 1 to channel 8, 1.10 dB from port 2 to port 7, 0.66 dB from port 3 to port 6, and 5.14 dB from port 4 to port 5 for the MDM transmission compared with the received optical power for the B2B transmission at an identical BER. Fig. 6(b) shows that the eye diagrams. Again, clear eye diagrams can be observed for B2B, single channel and four-mode MDM operation, which confirms the effectiveness of the system for MDM PAM-4 signal transmission using the fabricated MDM circuit. Again, the eyes for the channels from port 1 to port 8 and from port 4 to port 5 are relatively less opened due to higher channel crosstalks.

Thanks to the broad bandwidth and high fabrication tolerance provided by the directional couplers on the rib waveguides, the fabricated MDM circuit can support much higher data rate. The data rate demonstrated in the experiment is limited by the IM and PD due to their limited bandwidths. This successful demonstration of the on-chip MDM circuit paves the way for the implementation of a silicon photonic mode-selective lantern, which can find applications such as MDM enabled radio-over-fiber transmission system based on few- or multi- mode fiber [37], [38].

IV. Conclusion

A silicon photonic integrated four-channel MDM circuit was designed, fabricated and evaluated, and its use for short-reach optical communications was demonstrated. To make the circuit have a small size and support broadband operation, the mode multiplexer and demultiplexer were realized with the use of cascaded asymmetrical directional couplers on rib waveguides. By incorporating the fabricated MDM circuit in an optical communications system, a 4×10 GBaud/s on-chip MDM OOK and PAM-4 signal transmission was experimentally demonstrated. The performance of the transmission system using the MDM circuit was evaluated experimentally by measuring the eye diagrams and evaluating the power penalties. For all the transmission channels, clear eye diagrams were observed. The power penalties for four-channel OOK transmission were 4.31, 2.38, 1.44 and 3.5 dB at a BER of 10^{-9}. For four-channel PAM-4 transmission, the power penalties were 7.98, 1.10, 0.66 and 5.14 dB. The required received optical power at a BER of the 7% overhead-hard decision FEC was −2.6 dBm. The use of the MDM circuit makes the data capacity highly increased.

Since the MDM circuit was implemented on a silicon photonic platform, the system holds great potential for full integration on a single chip.

Acknowledgment

The work was supported by the Natural Sciences and Engineering Research Council (NSERC) of Canada. We would also like to acknowledge the CMC Microsystems for the provision of services that have facilitated this research.

References

[1] G. Keiser, *Optical Fiber Communications*, New York: McGraw Hill, 2000.
[2] C. A. Brackett, "Dense wavelength division multiplexing networks: principles and applications," *IEEE J. Select. Areas Commun.*, vol. 8, no. 6, pp. 948–964, Aug. 1990.
[3] S. L. Jansen, I. Morita, T.C. Schenk, and H. Tanaka, "Long-haul transmission of 16 × 52.5 Gbits/s polarization-division-multiplexed OFDM enabled by MIMO processing," *J. Opt. Netw.*, vol. 7, no. 2, pp. 173–182, Feb. 2008.
[4] I. Fatadin, D. Ives, and S. J. Savory, "Laser Linewidth tolerance for 16-QAM coherent optical systems using QPSK partitioning," *IEEE Photon. Technol. Lett.*, vol. 22, no. 9, pp. 631–633, May 2010.
[5] E. Ip, A. Lau, D. J. F. Barros, and J. M. Kahn, "Coherent detection in optical fiber systems," *Opt. Express*, vol. 16, no. 2, pp. 753–791, Jan. 2008.
[6] D. J. Richardson, J. M. Fini, and L. E. Nelson, "Space-division multiplexing in optical fibres," *Nature Photon.*, vol. 7, no. 5, pp. 354–362, Apr. 2013.
[7] R. G. H. van Uden *et al.*, "Ultra-high-density spatial division multiplexing with a few-mode multicore fibre," *Nature Photon.*, vol. 8, no. 10, pp. 865–870, Oct. 2014.
[8] B. Stern *et al.*, "On-chip mode-division multiplexing switch," *Optica*, vol. 2, no. 6, pp. 530–535, Jun. 2015.
[9] Y. Ding *et al.*, "On-chip two-mode division multiplexing using tapered directional coupler-based mode multiplexer and demultiplexer," *Opt. Express*, vol. 21, no. 8, pp. 10376–10382, Apr. 2013.
[10] Y. Sun, Y. Xiong, and W. N. Ye, "Experimental demonstration of a two-mode (de)multiplexer based on a taper-etched directional coupler," *Opt. Lett.*, vol. 41, no.16, pp. 3743–3746, Aug. 2016.
[11] T. Pan and S. Tseng, "Short and robust silicon mode (de)multiplexers using shortcuts to adiabaticity," *Opt. Express*, vol. 23, no. 8, pp. 10405–10412, Apr. 2015.
[12] J. Wang *et al.*, "Broadband and fabrication-tolerant on-chip scalable mode-division multiplexing based on mode-evolution counter-tapered couplers," *Opt. Lett.*, vol. 40, no. 9, pp. 1956–1959, May 2015.
[13] J. B. Driscoll *et al.*, "Asymmetric Y junctions in silicon waveguides for on-chip mode-division multiplexing," *Opt. Lett.*, vol. 38, no. 11, pp. 1854–1856, Jun. 2013.
[14] S. Bagheri and W. M. J. Green, "Silicon-on-insulator mode-selective add-drop unit for on-chip mode-division multiplexing," in *Proc. 2009 6th IEEE Int. Conf. Group IV Photon.*, San Francisco, CA, 2009, pp. 166–168.
[15] L. F. Frellsen *et al.*, "Topology-optimized silicon photonic wire mode (de)multiplexer." *Proc. SPIE*, vol. 9367, Feb. 2015.
[16] L. F. Frellsen *et al.*, "Topology optimized design for silicon-on-insulator mode converter," in *Proc. 2015 IEEE Photon. Conf. (IPC)*, Reston, VA, 2015, pp. 162–163.
[17] D. P. Galacho *et al.*, "Mode converters based on periodically perturbed waveguides for mode division multiplexing," in *Proc. SPIE 10686, Silicon Photon.: From Fundam. Res. Manuf.*, 106860R, May 2018.
[18] D. P. Galacho *et al.*, "Integrated mode converter for mode division multiplexing," in *Proc. SPIE 9891, Silicon Photon. Photonic Integr. Circuits V*, 98910B, May 2016.
[19] H. Jia *et al.*, "Optical switch compatible with wavelength division multiplexing and mode division multiplexing for photonic networks-on-chip," *Opt. Express*, vol. 25, no. 17, pp. 20698–20707, Aug. 2017.
[20] S. Chang *et al.*, "Mode- and wavelength-division multiplexed transmission using all-fiber mode multiplexer based on mode selective couplers," *Opt. Express*, vol. 23, no. 6, pp. 7164–7172, Mar. 2015.
[21] S. Zhang *et al.*, "Analysis of a modified adaptive least mean square frequency-domain algorithm for equalization in polarization division multiplexed-mode division multiplexed fiber transmission," in *Proc. 2017 Opto-Electronics and Commun. Conf. (OECC) Photon. Global Conf. (PGC)*, Singapore, 2017, pp. 1–3.
[22] J. B. Driscoll *et al.*, "Asymmetric Y-junctions in silicon waveguides for on-chip mode-division multiplexing," *Opt. Lett.*, vol. 38, no. 11, pp. 1854–1856, Jun. 2013.
[23] H. Chung, K. Lee, and S. Tseng, "Short and broadband silicon asymmetric Y-junction two-mode (de)multiplexer using fast quasiadiabatic dynamics," *Opt. Express*, vol. 25, no. 2, pp. 13626–13634, Jun. 2017.
[24] J. Wang, S. He, and D. Dai, "On-chip silicon 8-channel hybrid (de)multiplexer enabling simultaneous mode- and polarization-division-multiplexing," *Laser Photon. Rev.*, vol. 8, no. 2, pp. L18–L22, Jan. 2014.
[25] D. Dai, J. Wang, and Y. Shi, "Silicon mode (de)multiplexer enabling high capacity photonic networks-on-chip with a single-wavelength-carrier light," *Opt. Lett.*, vol. 38, no. 9, pp. 1422–1424, Feb. 2013.
[26] Y. Kawaguchi and K. Tsutsumi, "Mode multiplexing and demultiplexing devices using multimode interference couplers," *Electron. Lett.*, vol. 38, no. 25, pp. 1701–1702, Dec. 2002.
[27] T. Uematsu, Y. Ishizaka, Y. Kawaguchi, K. Saitoh, and M. Koshiba, "Design of a compact two-mode multi/demultiplexer consisting of multimode interference waveguides and a wavelength-insensitive phase shifter for mode-division multiplexing transmission," *J. Lightw. Technol.*, vol. 30, no. 15, pp. 2421–2426, Aug. 2012.
[28] D. Pérez-Galacho, D. Marris-Morini, A. Ortega-Moñux, J. G. Wangüemert-Pérez, and L. Vivien, "Add/drop mode-division multiplexer based on a mach–Zehnder interferometer and periodic waveguides," *IEEE Photon. J.*, vol. 7, no. 4, pp. 1–7, Aug. 2015
[29] S. Ohta *et al.*, "Si-based Mach-Zehnder wavelength/mode multi/demultiplexer for a WDM/MDM transmission system," *Opt. Express*, vol. 26, no. 12, pp. 15211–15220, Jun. 2018.
[30] B. A. Dorin and W. N. Ye, "Two-mode division multiplexing in a silicon-on-insulator ring resonator," *Opt. Express*, vol. 22, no. 4, pp. 4547–4558, Feb. 2014.
[31] L.-W. Luo *et al.*, "WDM-compatible mode-division multiplexing on a silicon chip," *Nature Commun.*, vol. 5, p. 3069, Jan. 2014.
[32] N. Riesen and J. D. Love, "Design of mode-sorting asymmetric Y-junctions," *Appl. Opt.*, vol. 51, no. 15, pp. 2778–2783, May 2012.
[33] L. Han *et al.*, "Two-mode de/multiplexer based on multimode interference couplers with a tilted joint as phase shifter," *Opt. Lett.*, vol. 40, no. 4, pp. 518–521, Feb. 2015.
[34] Y. Hsu *et al.*, "2.6 Tbit/s on-chip optical interconnect supporting mode-division-multiplexing and PAM-4 Signal," *IEEE Photon. Technol. Lett.*, vol. 30, no. 11, pp. 1052–1055, Jun. 2018.
[35] D. Dai *et al.*, "10-channel mode (de)multiplexer with dual polarizations," *Laser Photon. Rev.*, vol. 12, no. 1, p. 1700109, Nov. 2017.
[36] G. B. Cao, F. Gao, J. Jiang, and F. Zhang, "Directional couplers realized on silicon-on-insulator," *IEEE Photon. Technol. Lett.*, vol. 17, no. 8, pp. 1671–1673, Aug. 2005.
[37] S. G. Leon-Saval *et al.*, "Mode-selective photonic lanterns for space-division multiplexing," *Opt. Express*, vol. 22, no. 1, pp. 1036–1044, Jan. 2014.
[38] G. S. D. Gordon, M. J. Crisp, R. V. Penty, T. D. Wilkinson, and I. H. White, "Feasibility demonstration of a mode-division multiplexed MIMO-enabled radio-over-fiber distributed antenna system," *J. Lightw. Technol.*, vol. 32, no. 20, pp. 3521–3528, Oct. 2014.

Weifeng Zhang (S'12–M'17) received the B.Eng. degree in electronic science and technology from Xi'an Jiaotong University, Xi'an, China, in 2008, the M.A.Sc. degree in electrical engineering from the Politecnico di Torino, Torino, Italy, in 2011, and the Ph.D. degree in electrical engineering from the University of Ottawa, Ottawa, ON, Canada, in 2017. He is currently a Postdoctoral Fellow with the Microwave Photonics Research Laboratory, School of Electrical Engineering and Computer Science, University of Ottawa.

His current research interests include silicon photonics and its applications in microwave photonics.

Houman Ghorbani received the B.Sc. degree in electrical engineering from the University of Tabriz, Tabriz, Iran, in 2010 and the M.A.Sc. degree in electrical engineering from the Amirkabir University of Technology, Tehran, Iran, in 2014. He is currently working toward the Ph.D. degree in electrical engineering with the University of Ottawa, Ottawa, ON, Canada.

Tong Shao (M'12) received the B.Eng. and M.Eng. degrees from Tsinghua University, Beijing, China, in 2007 and 2009, respectively, and the Ph.D. degree from the Institut Polytechnique de Grenoble (INP-Grenoble), Grenoble, France, in 2012. From August 2012 to July 2013, he was with the University of Ottawa, as a Postdoctoral Fellow. From September 2013 to July 2015, he was with the Radio and Optical Communication Lab, Rince Institute, Dublin City University, Ireland. In August 2015, he joined Lumentum, Ottawa, Canada as a Senior Optical Engineer. His research interests include advanced optical transmission systems and radio over fiber technique. In 2015, he was awarded the Marie Skłodowska-Curie Individual Fellowship

Jianping Yao (M'99–SM'01–F'12) received the Ph.D. degree in electrical engineering from the Université de Toulon et du Var, Toulon, France, in December 1997. He is a Distinguished University Professor and University Research Chair with the School of Electrical Engineering and Computer Science, University of Ottawa, Ottawa, ON, Canada. From 1998 to 2001, he was with the School of Electrical and Electronic Engineering, Nanyang Technological University, Singapore, as an Assistant Professor. In December 2001, he joined the School of Electrical Engineering and Computer Science, University of Ottawa, as an Assistant Professor, where he was promoted to an Associate Professor in May 2003, and a Full Professor in May 2006. He was appointed University Research Chair in Microwave Photonics in 2007. In June 2016, he was conferred the title of Distinguished University Professor of the University of Ottawa. From July 2007 to June 2010 and July 2013 to June 2016, he was the Director of the Ottawa-Carleton Institute for Electrical and Computer Engineering.

He has authored or coauthored more than 600 research papers including more than 360 papers in peer-reviewed journals and more than 260 papers in conference proceedings. He is the Editor-in-Chief for the IEEE PHOTONICS TECHNOLOGY LETTERS, a former Topical Editor for *Optics Letters*, an Associate Editor for *Science Bulletin*, a Steering Committee Member for the IEEE JOURNAL OF LIGHTWAVE TECHNOLOGY, and an Advisory Editorial Board member for *Optics Communications*. He was a Guest Editor of a Focus Issue on Microwave Photonics in *Optics Express* in 2013, a Lead-Editor of a Feature Issue on Microwave Photonics in *Photonics Research* in 2014, and a Guest Editor of a special issue on Microwave Photonics in IEEE/OSA JOURNAL OF LIGHTWAVE TECHNOLOGY in 2018. He is currently the Technical Committee Chair of IEEE MTT-3 Microwave Photonics and an elected member of the Board of Governors of the IEEE Photonics Society (2019–2021). He was a member of the European Research Council Consolidator Grant Panel in 2016 and 2018, the Qualitative Evaluation Panel in 2017, and a panelist of the National Science Foundation Career Awards Panel in 2016. He has also served as a Chair of a number of international conferences, symposia, and workshops, including the Vice Technical Program Committee (TPC) Chair of the 2007 IEEE Topical Meeting on Microwave Photonics, a TPC Co-Chair of the 2009 and 2010 Asia-Pacific Microwave Photonics Conference, a TPC Chair of the high-speed and broadband wireless technologies subcommittee of the IEEE Radio Wireless Symposium 2009-2012, a TPC Chair of the microwave photonics subcommittee of the IEEE Photonics Society Annual Meeting 2009, a TPC Chair of the 2010 IEEE Topical Meeting on Microwave Photonics, a General Co-Chair of the 2011 IEEE Topical Meeting on Microwave Photonics, a TPC Co-Chair of the 2014 IEEE Topical Meetings on Microwave Photonics, a General Co-Chair of the 2015 and 2017 IEEE Topical Meeting on Microwave Photonics, and a General Chair of the 2019 IEEE Topical Meeting on Microwave Photonics. He also served as a committee member for a number of international conferences, such as IPC, OFC, CLEO, BGPP, and MWP. He received the 2005 International Creative Research Award of the University of Ottawa. He was the recipient of the 2007 George S. Glinski Award for Excellence in Research. In 2008, he was awarded a Natural Sciences and Engineering Research Council of Canada Discovery Accelerator Supplements Award. He was selected to receive an inaugural OSA Outstanding Reviewer Award in 2012 and was one of the top ten reviewers for the IEEE/OSA JOURNAL OF LIGHTWAVE TECHNOLOGY 2015–2016. He was an IEEE MTT-S Distinguished Microwave Lecturer for 2013–2015. He received the 2017–2018 Award for Excellence in Research of the University of Ottawa, and was the recipient of the 2018 R.A. Fessenden Silver Medal from IEEE Canada.

He is a Registered Professional Engineer of Ontario. He is a fellow of the Optical Society of America, the Canadian Academy of Engineering, and the Royal Society of Canada.